

# Long time self-modulation of nonlinear electromagnetic wave in two-dimensional cavity

Kazunori Shibata

*Institute of Laser Engineering, Osaka University,  
2-6 Yamada-Oka, Suita, Osaka 565-0871 Japan*

(Dated: February 4, 2022)

arXiv:2202.01476v1 [physics.optics] 3 Feb 2022

## Abstract

The vacuum is expected to exhibit electromagnetic nonlinearity. We demonstrate the properties of nonlinear electromagnetic wave in a two-dimensional rectangular cavity by calculating the nonlinear correction for two classical standing waves. We apply the linear approximation in a short timescale. A part of the nonlinear correction increases with time. In particular, a one-dimensional second harmonic grows if the cavity size satisfies a specific condition. We also analyze the nonlinear electromagnetic wave in a timescale longer than the applicable limit of the linear approximation. We formulate the self-modulation of the amplitude and phase, including the effect of static magnetic flux density. In the viewpoint of energy flow between the two modes of the standing wave, the behavior of nonlinear electromagnetic wave can be classified into three types. Namely, the energy flow keeps oscillating, eventually decreases to zero, or never occurs.

## I. INTRODUCTION

An electromagnetic field in the classical vacuum is well described by the linear Maxwell's equations. After the advent of quantum field theory in the 20th century, a correction to the classical electromagnetic field has emerged. For example, a correction by virtual pairs of electron and positron in quantum electrodynamics is known as the Heisenberg-Euler model [1][2]. Another famous model is the Born-Infeld model [3] which is derived by an analogy to the theory of relativity. These corrections yield nonlinear Maxwell's equations.

Such a nonlinear correction has been pointed out to affect various phenomena, such as the Wichmann-Kroll correction to the Lamb shift [4] and a correction to the energy levels of a hydrogen atom [5][6][7][8]. However, an experimental verification has yet to succeed.

Various experiments and experimental proposals have been designed to verify the electromagnetic vacuum nonlinearity. A focusing of a strong laser beam is typically considered [9]. Such an attempt aims to generate a nonlinear effect by instantaneously achieving an extremely large intensity [10][11] [12]. However, a strong laser is not the only approach. For example, nonlinear behaviors in a cavity system [13][14] [15][16] [17] [18][19], a waveguide [14][20] [21], and a ring laser [22] have been calculated. In particular, several experiments using a cavity have been performed to detect vacuum birefringence [23][24][25] [26][27] [28][29].

A cavity is capable of confining an electromagnetic wave in a long time compared to the timescale of laser focusing. A characteristic behavior of nonlinear electromagnetic wave can

appear in a long timescale by accumulating an instantaneously small nonlinear effect, as reported in a one-dimensional system [30]. However, it is hard to predict the behavior of nonlinear electromagnetic waves in a two- or three-dimensional cavity because a physical phenomenon generally changes its behavior depending on the spatial dimension. Thusly, it is worth clarifying theoretically the property of nonlinear electromagnetic waves for future experiments.

In this study, we analyze a nonlinear electromagnetic wave in a two-dimensional rectangular cavity. First, we employ the linear approximation and clarify the condition that the nonlinear corrective term can increase with time. Then, we elucidate the leading term of nonlinear electromagnetic waves in a longer timescale than the applicable range of the linear approximation. As a characteristic behavior in the two-dimensional cavity, we report that a second harmonic can increase with time depending on the cavity size.

## II. NOTATION, SYSTEM, AND CLASSICAL TERM

The electromagnetic fields are normalized by the electric constant  $\varepsilon_0$  and magnetic constant  $\mu_0$  as follows. The electric field  $\mathbf{E}$  and vacuum polarization  $\mathbf{P}$  are multiplied by  $\varepsilon_0^{1/2}$  and  $\varepsilon_0^{-1/2}$ , respectively. Similarly, the magnetic flux density  $\mathbf{B}$  and vacuum magnetization  $\mathbf{M}$  are multiplied by  $\mu_0^{-1/2}$  and  $\mu_0^{1/2}$ , respectively. We suppose  $\mathbf{E}$  and  $\mathbf{B}$  to be of class  $C^1$ .

We consider the simplest nonlinear Lagrangian density  $L$  in the Plebański class [31] as

$$L = \frac{1}{2}F + C_{2,0}F^2 + C_{0,2}G^2. \quad (1)$$

This form is frequently used because it can be an effective Lagrangian if the electromagnetic fields are not extremely strong.  $C_{2,0}$  and  $C_{0,2}$  are the nonlinear parameters, *e.g.*, their values in the Heisenberg-Euler model are  $C_{2,0} = 1.665 \times 10^{-30}(\text{m}^3/\text{J})$  and  $C_{0,2} = 7C_{2,0}$ , respectively[2][32] [33]. The polarization  $\mathbf{P}$  and magnetization  $\mathbf{M}$  of vacuum are defined as

$$\begin{aligned} \mathbf{P} &= 4C_{2,0}F\mathbf{E} + 2C_{0,2}G\mathbf{B}, \\ \mathbf{M} &= -4C_{2,0}F\mathbf{B} + 2C_{0,2}G\mathbf{E}, \end{aligned} \quad (2)$$

respectively. The charge  $\rho$  and current  $\mathbf{j}$  of vacuum are composed of electromagnetic field itself as

$$\begin{aligned} \rho &= -\nabla \cdot \mathbf{P}, \\ \mathbf{j} &= c^{-1}\partial_t\mathbf{P} + \nabla \times \mathbf{M}, \end{aligned} \quad (3)$$

where  $c$  is the speed of light and  $\partial_t$  denotes the partial differentiation with respect to time  $t$ . The nonlinear Maxwell's equations are given by

$$\begin{aligned}
\nabla \cdot \mathbf{B} &= 0, \\
\nabla \times \mathbf{E} + c^{-1} \partial_t \mathbf{B} &= \mathbf{0}, \\
\nabla \cdot \mathbf{E} &= \rho, \\
\nabla \times \mathbf{B} - c^{-1} \partial_t \mathbf{E} &= \mathbf{j}.
\end{aligned} \tag{4}$$

The nonlinearity appears in the form of  $\rho$  and  $\mathbf{j}$ .

The physical system we treat is a two-dimensional cavity whose domain is set to  $0 \leq x \leq \ell_1, 0 \leq y \leq \ell_2$  and the boundary is supposed to be a perfect conductor mirror. On the surface of the mirror, a static magnetic flux density  $\mathbf{B}_s = (B_{sx}, B_{sy}, B_{sz})$  can exist. The boundary conditions are given by

$$\begin{aligned}
E_y(0, y, t) &= 0, & E_y(\ell_1, y, t) &= 0, \\
E_z(0, y, t) &= 0, & E_z(\ell_1, y, t) &= 0, \\
B_x(0, y, t) &= B_{sx}, & B_x(\ell_1, y, t) &= B_{sx}, \\
E_x(x, 0, t) &= 0, & E_x(x, \ell_2, t) &= 0, \\
E_z(x, 0, t) &= 0, & E_z(x, \ell_2, t) &= 0, \\
B_y(x, 0, t) &= B_{sy}, & B_y(x, \ell_2, t) &= B_{sy}.
\end{aligned} \tag{5}$$

Here we describe a classical standing wave that can exist in the cavity. Let  $k > 0$  be the magnitude of the wave vector. The wave direction is expressed by an angle  $\theta$ . Using two natural numbers  $n_1$  and  $n_2$ ,  $\theta$  satisfies  $\cos \theta = n_1 \pi / (k \ell_1)$  and  $\sin \theta = n_2 \pi / (k \ell_2)$  because of the boundary conditions. The frequency is given by  $\omega = ck$ . There are two modes of the standing wave with this wave vector. Let  $A_1, A_2 \geq 0$  be the amplitudes of respective modes and  $\Phi$  be the relative phase. At least one of  $A_1$  or  $A_2$  are supposed to be nonzero. We abbreviate to  $X = (k \cos \theta)x, Y = (k \sin \theta)y$ , and  $T = \omega t$ . The classical electromagnetic fields  $\mathbf{E}_c$  and  $\mathbf{B}_c$  are generated at a certain negative time and their values at  $t \geq 0$  are given

by

$$\begin{aligned} \mathbf{E}_c &= \begin{pmatrix} -A_1 \sin \theta \cos X \sin Y \sin T \\ A_1 \cos \theta \sin X \cos Y \sin T \\ A_2 \sin X \sin Y \sin(T + \Phi) \end{pmatrix}, \\ \mathbf{B}_c &= \begin{pmatrix} A_2 \sin \theta \sin X \cos Y \cos(T + \Phi) \\ -A_2 \cos \theta \cos X \sin Y \cos(T + \Phi) \\ A_1 \cos X \cos Y \cos T \end{pmatrix} + \mathbf{B}_s, \end{aligned} \quad (6)$$

where we set  $\mathbf{B}_s$  to be constant. These fields satisfy the classical linear Maxwell's equations. However, they do not necessarily satisfy the nonlinear Maxwell's equations. The difference between the total electromagnetic field and the classical term is referred to as the corrective term and expressed by a subscript  $n$ . Thus, we can express as  $\mathbf{E} = \mathbf{E}_c + \mathbf{E}_n$  and  $\mathbf{B} = \mathbf{B}_c + \mathbf{B}_n$ . Our concern is to calculate the corrective term, in particular, its magnitude.

We first apply a linear approximation by assuming that the corrective term is much smaller than the classical term. The corrective term within the range of the linear approximation is especially called ‘‘minimum corrective term’’ and we attach a superscript (0) in addition to a subscript  $n$ . The minimum corrective term is the first-order correction of the regular perturbation. We expect that the minimum corrective term is a good approximation of the exact corrective term in a short timescale, *i.e.*,  $\mathbf{E}_n^{(0)} \approx \mathbf{E}_n$ . In the following calculations, at least one of  $B_{sx}$  and  $B_{sy}$  is zero to avoid the situation of no solution [34].

### III. LINEAR APPROXIMATION

In the linear approximation, the charge and current in Eq. (3) are composed only of the classical term. We express them as  $\rho_c$  and  $\mathbf{j}_c$ , respectively. The minimum corrective term is generated by these wave sources and satisfies the following equations:

$$\begin{aligned} \nabla \cdot \mathbf{B}_n^{(0)} &= 0, \\ \nabla \times \mathbf{E}_n^{(0)} + c^{-1} \partial_t \mathbf{B}_n^{(0)} &= \mathbf{0}, \\ \nabla \cdot \mathbf{E}_n^{(0)} &= \rho_c, \\ \nabla \times \mathbf{B}_n^{(0)} - c^{-1} \partial_t \mathbf{E}_n^{(0)} &= \mathbf{j}_c. \end{aligned} \quad (7)$$

The boundary conditions for the minimum corrective term are given according to the conditions in Eq. (5).

The minimum corrective term is a sum of the homogeneous and special solutions of Eq. (7). In the framework of classical electromagnetism, the homogeneous solution is proven not to increase with time. Furthermore, the initial distribution of minimum corrective term affects only the homogeneous solution. Therefore, it is sufficient to elucidate the behavior of the special solution to discuss the magnitude of the minimum corrective term.

### A. Resonant increase

A part of the minimum corrective term resonantly increases with time. We express such a part by  $\mathbf{E}_{\text{reso}}$  and  $\mathbf{B}_{\text{reso}}$ . By defining constants

$$\begin{aligned}\Gamma &= \frac{1}{8}C_{2,0}(4 - \sin^2 2\theta), \\ \Gamma_1 &= 4C_{2,0}B_{sz}^2 + C_{0,2}(B_{sx}^2 \sin^2 \theta + B_{sy}^2 \cos^2 \theta), \\ \Gamma_2 &= 4C_{2,0}(B_{sx}^2 \sin^2 \theta + B_{sy}^2 \cos^2 \theta) + C_{0,2}B_{sz}^2, \\ \tilde{\Gamma} &= -\frac{1}{8}(3C_{2,0} \sin^2 2\theta - C_{0,2}),\end{aligned}\tag{8}$$

and using

$$\begin{aligned}f_1 &= (\Gamma - \tilde{\Gamma})A_1A_2^2 \sin \Phi \cos \Phi, \\ g_1 &= -\Gamma_1A_1 - 3\Gamma A_1^3 - \Gamma A_1A_2^2 \cos^2 \Phi - \tilde{\Gamma}A_1A_2^2 \sin^2 \Phi, \\ p_1 &= (\Gamma_2 + 3\Gamma A_2^2 + \tilde{\Gamma}A_1^2) A_2 \sin \Phi, \\ q_1 &= -(\Gamma_2 + 3\Gamma A_2^2 + \Gamma A_1^2) A_2 \cos \Phi,\end{aligned}\tag{9}$$

we obtain

$$\begin{aligned}\mathbf{E}_{\text{reso}} &= T \begin{pmatrix} -\sin \theta (f_1 \sin T + g_1 \cos T) \cos X \sin Y \\ \cos \theta (f_1 \sin T + g_1 \cos T) \sin X \cos Y \\ (p_1 \sin T + q_1 \cos T) \sin X \sin Y \end{pmatrix}, \\ \mathbf{B}_{\text{reso}} &= T \begin{pmatrix} \sin \theta (-q_1 \sin T + p_1 \cos T) \sin X \cos Y \\ -\cos \theta (-q_1 \sin T + p_1 \cos T) \cos X \sin Y \\ (-g_1 \sin T + f_1 \cos T) \cos X \cos Y \end{pmatrix}.\end{aligned}\tag{10}$$

The resonant terms are partially calculated in Ref. [19]. The behavior that is proportional to time  $T$  is the same as the resonance discussed in a one-dimensional system [18][19]. One can see that there is an upper limit in the applicable time of the linear approximation because the resonant terms in Eq. (10) must be much smaller than the classical term.

## B. Another increase

In the two-dimensional system, there can be an increasing solution which possesses a different property. The essential origin is a spatially uniform current. In the present system, a part of  $\mathbf{j}_c$  is given by

$$\mathbf{j}_{\text{uni}} = -\frac{k}{4}(4C_{2,0} - C_{0,2})A_1A_2 \sin 2\theta \cos(2T + \Phi) \begin{pmatrix} B_{sy} \\ B_{sx} \\ 0 \end{pmatrix}, \quad (11)$$

where the corresponding charge is zero. All other terms in  $\mathbf{j}_c$  depend on  $x$  or  $y$ . Such a uniform current is characteristic to electromagnetic nonlinear interaction, in other words, it cannot be realized by a matter. The corresponding minimum corrective term must satisfy the boundary conditions and be bounded at  $T = 0$ . Such a solution is obtained as

$$\begin{aligned} E_x &= B_{sy} \left[ -\frac{1}{2}(1 - \cos 2ky) \sin(2T + \Phi) + K_1(T - ky) - K_1(T + ky) \right], \\ E_y &= B_{sx} \left[ -\frac{1}{2}(1 - \cos 2kx) \sin(2T + \Phi) + K_2(T - kx) - K_2(T + kx) \right], \\ B_z &= B_{sx} \left[ -\frac{1}{2} \sin 2kx \cos(2T + \Phi) + K_2(T - kx) + K_2(T + kx) \right] \\ &\quad - B_{sy} \left[ -\frac{1}{2} \sin 2ky \cos(2T + \Phi) + K_1(T - ky) + K_1(T + ky) \right], \end{aligned} \quad (12)$$

$E_z = 0$ ,  $B_x = 0$ , and  $B_y = 0$ , where the common coefficient  $-(1/4)(4C_{2,0} - C_{0,2})A_1A_2 \sin 2\theta$  is omitted. The function  $K_1(\bar{T})$  is defined at  $\bar{T} \geq -k\ell_2$  and given as

$$K_1(\bar{T}) = \begin{cases} -\frac{1}{4} [\sin(2\bar{T} + \Phi) - \sin \Phi] + \frac{1}{2} [\tilde{B}_1(-k^{-1}\bar{T}) + \tilde{E}_1(-k^{-1}\bar{T})] & (-k\ell_2 \leq \bar{T} \leq 0) \\ \frac{1}{4} [\sin(2\bar{T} + \Phi) - \sin \Phi] + \frac{1}{2} [\tilde{B}_1(k^{-1}\bar{T}) - \tilde{E}_1(k^{-1}\bar{T})] & (0 \leq \bar{T} < k\ell_2) \\ K_1(\bar{T} - 2k\ell_2) - \frac{1}{2}(1 - \cos 2k\ell_2) \sin(2\bar{T} - 2k\ell_2 + \Phi) & (\bar{T} \geq k\ell_2), \end{cases} \quad (13)$$

where functions  $\tilde{E}_1(y)$  and  $\tilde{B}_1(y)$  express the initial distribution of the special solution and their domain is  $y \in [0, \ell_2]$ . The function  $K_2(\bar{T})$  is defined at  $\bar{T} \geq -k\ell_1$  and is obtained by replacing  $\tilde{E}_1$ ,  $\tilde{B}_1$ , and  $\ell_2$  in the above equation by  $\tilde{E}_2$ ,  $\tilde{B}_2$ , and  $\ell_1$ , respectively. The domain of  $\tilde{E}_2(x)$  and  $\tilde{B}_2(x)$  is  $x \in [0, \ell_1]$ . These  $\tilde{E}_1(y)$ ,  $\tilde{B}_1(y)$ ,  $\tilde{E}_2(x)$ , and  $\tilde{B}_2(x)$  are supposed to be

of class  $C^1$  and satisfy

$$\begin{aligned}
\tilde{E}_1(0) &= \tilde{E}_1(\ell_2) = 0, \\
\tilde{B}'_1(0) &= \tilde{B}'_1(\ell_2) = -k \cos \Phi, \\
\tilde{E}_2(0) &= \tilde{E}_2(\ell_1) = 0, \\
\tilde{B}'_2(0) &= \tilde{B}'_2(\ell_1) = -k \cos \Phi.
\end{aligned} \tag{14}$$

With these boundary values, we can confirm that  $K_1, K_2$ , and the minimum corrective term to be of class  $C^1$ . Furthermore, if  $\tilde{E}_1(y), \tilde{B}_1(y), \tilde{E}_2(x)$ , and  $\tilde{B}_2(x)$  are of class  $C^2$  and satisfy  $\tilde{E}_1''(0) = \tilde{E}_1''(\ell_2) = \tilde{E}_2''(0) = \tilde{E}_2''(\ell_1) = -2k^2 \sin \Phi$ , then  $K_1, K_2$ , and the minimum corrective term are of class  $C^2$ .

It will be worth noting that the minimum corrective term generated by the uniform current has a property that its time evolution varies with the cavity size. We fix  $y$  and demonstrate the time-evolution of  $E_x$  in the case of  $B_{sy} \neq 0$ . Using a certain  $t_0 \in [0, 2c^{-1}\ell_2)$  and a natural number  $n$ , a general time  $t \geq 0$  can be expressed as  $t = t_0 + 2nc^{-1}\ell_2$ . Thus, we obtain

$$\begin{aligned}
E_x(y, t) &= E_x(y, t_0) - \frac{B_{sy}}{2}(1 - \cos 2ky)[\sin(2\omega t_0 + 4nkl_2 + \Phi) - \sin(2\omega t_0 + \Phi)] \\
&\quad + B_{sy}(1 - \cos 2kl_2) \sum_{p=1}^n \cos[2\omega t_0 + (4p - 2)kl_2 + \Phi] \sin 2ky,
\end{aligned} \tag{15}$$

where the sum originates from the relationship in Eq. (13). The first and second terms in the right-hand side do not increase with  $n$ , *i.e.*, they are bounded with respect to time. However, the sum in the third term can increase with  $n$ . In fact, if  $\cos kl_2 = 0$ , then the third term becomes  $2nB_{sy} \cos(2\omega t_0 - 2kl_2 + \Phi) \sin 2ky$ , which clearly increases with  $n$ . Figure 1 shows an example. If  $\cos kl_2 \neq 0$ , the third term is also bounded with respect to time.

Similar calculation shows that  $E_y$  can increase with time in the case of  $\cos kl_1 = 0$ . The one-dimensional second harmonic wave generated by the uniform current can increase with time only if the cavity size and wave number satisfy the specific conditions that  $\cos kl_1 = 0$  or  $\cos kl_2 = 0$ . Such a behavior is obviously different from the resonant increase.

### C. Applicable time of linear approximation

The linear approximation can be a good approximation only when the minimum corrective term is much smaller than the classical term. All terms of minimum corrective term other

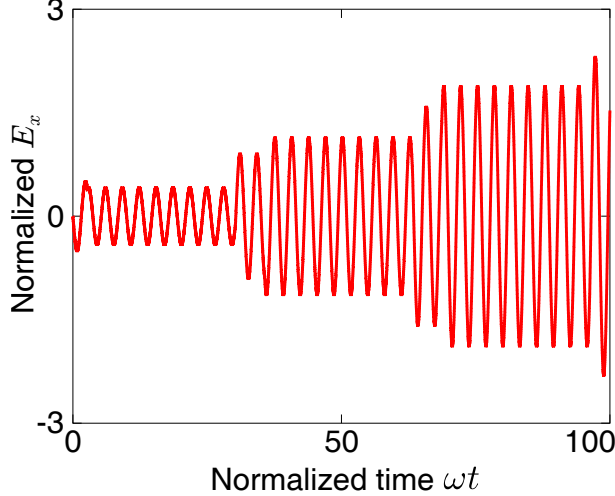


FIG. 1. Example of increasing second harmonic generated by the uniform current in the case of  $\cos k\ell_2 = 0$ . The electric field  $E_x$  is normalized by  $-(1/4)(4C_{2,0} - C_{0,2})A_1A_2B_{sy} \sin 2\theta$ . The parameters are set to  $k\ell_2 = 10.5\pi, ky = 2.718$ , and  $\Phi = 0$ . The graph is continuous but not differentiable at  $\omega t = \pm kx + nk\ell_2, n \in \mathbb{N}$  because we employ  $\tilde{E}_1 = 0$  and  $\tilde{B}_1 = 0$ .

than abovementioned do not increase with time. The amplitude of resonantly increasing term is about  $(C_{2,0} + C_{0,2})(A_1 + A_2 + B_s)^3\omega t$ . Similarly, that of the increasing term generated by the uniform current is about  $(C_{2,0} + C_{0,2})(A_1 + A_2 + B_s)^3(c/\ell_1)t$ , in the case of  $\cos k\ell_1 = 0$ . If we choose a typical size of the cavity as 10 (cm) and the standing wave to be visible light,  $\omega$  is larger than  $c/\ell_1$  by about 6 orders. It means that the resonant increase can appear much earlier. Therefore, we can evaluate the applicable time of the linear approximation by using only the resonantly increasing term, *i.e.*, if  $A_1, A_2 \neq 0$ ,

$$t \ll \omega^{-1} \min \left( \frac{A_1}{\sqrt{f_1^2 + g_1^2}}, \frac{A_2}{\sqrt{p_1^2 + q_1^2}} \right). \quad (16)$$

#### IV. LEADING PART IN LONG TIMESCALE

We investigate the behavior of nonlinear electromagnetic wave in a longer timescale than the applicable range of linear approximation. We discuss a condition or timescale where the increase of a second harmonic wave can be excluded.

A resonantly increasing part in Eq. (10) has the same spatial part as the corresponding classical term. Thus, if we calculate a higher-order correction by regarding the resonant part as a new wave source, the leading part of the higher-order correction should have the same

spatial part. Therefore, we can expect that the leading part of the nonlinear electromagnetic wave has the same spatial part as the classical term, even in the longer timescale. We express such a leading part as

$$\begin{aligned} \mathbf{E}^{(\text{lp})} &= \begin{pmatrix} -\sin\theta(f\sin T + g\cos T)\cos X\sin Y \\ \cos\theta(f\sin T + g\cos T)\sin X\cos Y \\ (p\sin T + q\cos T)\sin X\sin Y \end{pmatrix}, \\ \mathbf{B}^{(\text{lp})} &= \begin{pmatrix} \sin\theta(-q\sin T + p\cos T)\sin X\cos Y \\ -\cos\theta(-q\sin T + p\cos T)\cos X\sin Y \\ (-g\sin T + f\cos T)\cos X\cos Y \end{pmatrix} + \mathbf{B}_s, \end{aligned} \quad (17)$$

where the envelope functions  $f, g, p$ , and  $q$  depend only on the normalized time  $T$ . Our concern is to verify the assumption of the leading part and to calculate these envelope functions. Note that the classical term is also included in the leading part. Thus,  $\mathbf{E}^{(\text{lp})}$  and  $\mathbf{B}^{(\text{lp})}$  are of the order of  $A_1 + A_2 + B_s$ . In particular, the envelope functions are of the order of  $A_1 + A_2$ . All discarded terms are expected to be at most of the order of  $(C_{2,0} + C_{0,2})(A_1 + A_2 + B_s)^3 \ll A_1 + A_2$ . By substituting the leading part in the nonlinear Maxwell's equations in Eq. (4), we can see that the envelope functions should satisfy the following differential equations:

$$\begin{aligned} f' &= \Gamma_1 g + 3\Gamma(f^2 + g^2)g + (\Gamma - \tilde{\Gamma})fpq + \tilde{\Gamma}gp^2 + \Gamma gq^2, \\ g' &= -\Gamma_1 f - 3\Gamma(f^2 + g^2)f - \Gamma fp^2 - \tilde{\Gamma}fq^2 - (\Gamma - \tilde{\Gamma})gpq, \\ p' &= \Gamma_2 q + 3\Gamma(p^2 + q^2)q + (\Gamma - \tilde{\Gamma})fqp + \tilde{\Gamma}f^2q + \Gamma g^2q, \\ q' &= -\Gamma_2 p - 3\Gamma(p^2 + q^2)p - (\Gamma - \tilde{\Gamma})fgq - \Gamma f^2p - \tilde{\Gamma}g^2p. \end{aligned} \quad (18)$$

Note that these equations are closed with  $f, g, p$ , and  $q$ . The initial values are

$$f(0) = A_1, g(0) = 0, p(0) = A_2 \cos \Phi, q(0) = A_2 \sin \Phi. \quad (19)$$

We first check the appropriateness of the differential equations. By substituting the initial values in Eq. (19) into the right-hand side of Eq. (18), the results agree with the right-hand side of Eq. (9). Therefore, the solution of these differential equations can reproduce the resonant increase in the linear approximation. Furthermore, let

$$\mathcal{X} = f^2 + g^2 + p^2 + q^2, \quad (20)$$

we can see that the time differential of  $\mathcal{X}$  is always zero and therefore,  $\mathcal{X} = A_1^2 + A_2^2$  is a conservative quantity. The conservative quantity indicates that the leading part of the total electromagnetic energy in the cavity is preserved. Because of these two properties, it will be reasonable to expect that the electromagnetic field in a long timescale is well approximated by Eq. (17) and the time-evolution of  $f, g, p$ , and  $q$  is determined by Eq. (18). In the next section, we introduce a new function  $\alpha$  to perform the analysis in an easier way. In section 8, we return to the equations by showing that  $f, g, p$ , and  $q$  are determined once  $\alpha$  is obtained.

## V. THREE DIFFERENTIAL EQUATIONS FOR $\alpha, \beta$ , AND $\gamma$

We introduce three functions  $\alpha, \beta$ , and  $\gamma$  as

$$\begin{aligned}\alpha &= \frac{1}{\mathcal{X}}(f^2 + g^2), \\ \beta &= \frac{1}{\mathcal{X}}(fp + gq), \\ \gamma &= \frac{1}{\mathcal{X}}(fq - gp).\end{aligned}\tag{21}$$

We also introduce three constants as

$$\begin{aligned}c_1 &= (\tilde{\Gamma} - \Gamma)\mathcal{X}, \\ c_2 &= (3\Gamma - \tilde{\Gamma})\mathcal{X}, \\ \xi &= \Gamma_2 - \Gamma_1 + (3\Gamma - \tilde{\Gamma})\mathcal{X}.\end{aligned}\tag{22}$$

Using Eq. (18), we obtain three differential equations for  $\alpha, \beta$ , and  $\gamma$  as

$$\begin{aligned}\alpha' &= -2c_1\beta\gamma, \\ \beta' &= (\xi - 2c_2\alpha)\gamma, \\ \gamma' &= -(\xi + c_1)\beta + 2(c_1 + c_2)\alpha\beta.\end{aligned}\tag{23}$$

Note that these differential equations are closed by the three functions. The initial values are given by

$$\alpha(0) = \frac{A_1^2}{\mathcal{X}}, \quad \beta(0) = \frac{A_1 A_2}{\mathcal{X}} \cos \Phi, \quad \gamma(0) = \frac{A_1 A_2}{\mathcal{X}} \sin \Phi.\tag{24}$$

It is clear from the definition that all  $\alpha, \beta$ , and  $\gamma$  are bounded and the right-hand sides of Eq. (23) are proven to be Lipschitz continuous. Therefore, a unique solution exists for the initial values.

We introduce a constant of integration  $Z$  by integrating the second line in Eq. (23) after multiplying by  $-2c_1\beta$ . Let

$$\begin{aligned} P_1(\alpha) &= c_2\alpha^2 - \xi\alpha - Z, \\ P_2(\alpha) &= -(c_1 + c_2)\alpha^2 + (\xi + c_1)\alpha + Z, \end{aligned} \tag{25}$$

we obtain

$$c_1\beta^2 = P_1(\alpha), \quad c_1\gamma^2 = P_2(\alpha). \tag{26}$$

We can also see

$$P_1(\alpha) + P_2(\alpha) = c_1\alpha(1 - \alpha), \tag{27}$$

and

$$\alpha'^2 = 4P_1(\alpha)P_2(\alpha). \tag{28}$$

We can immediately obtain  $\alpha$  from the last equation if the sign of  $\alpha'$  does not change. Even though the sign of  $\alpha'$  can change, we can obtain a second order differential equation that only includes  $\alpha$ , which must be easier to solve than Eq. (23). Therefore, we focus on  $\alpha$ . As we show later, the leading part of the electromagnetic field can be obtained once  $\alpha$  is calculated.

Because of Eq. (28), the range of possible  $\alpha$  is limited to satisfy  $P_1P_2 \geq 0$ . Thus, we assign symbols for the roots of  $P_1$  and  $P_2$ . They are given by

$$\begin{aligned} \alpha_{1\pm} &= \frac{\xi}{2c_2} \pm \frac{1}{2c_2} \sqrt{\xi^2 + 4c_2Z}, \\ \alpha_{2\pm} &= \frac{\xi + c_1}{2(c_1 + c_2)} \pm \frac{1}{2(c_1 + c_2)} \sqrt{(\xi + c_1)^2 + 4(c_1 + c_2)Z}, \end{aligned} \tag{29}$$

respectively.

## VI. RANGE OF PARAMETERS $c_1, c_2, \xi$ , AND $Z$

Since the parameters  $c_1$  and  $c_2$  appear in the coefficients of the highest degrees of  $P_1$  and  $P_2$ , their signs are especially important. In the Heisenberg-Euler model, they are positive as  $c_1 \geq (1/8)C_{2,0}\mathcal{X} > 0$  and  $c_2 = (5/8)C_{2,0}\mathcal{X} > 0$ . Thus, we fix them to be positive constants, *i.e.*, we fix the nonlinear vacuum model,  $\mathcal{X} = A_1^2 + A_2^2$ , and  $\theta$ . In this case,  $P_1$  is convex downward and  $P_2$  is convex upward. Equation (27) shows that  $\alpha \neq 0, 1$  is never a common root of  $P_1$  and  $P_2$ .

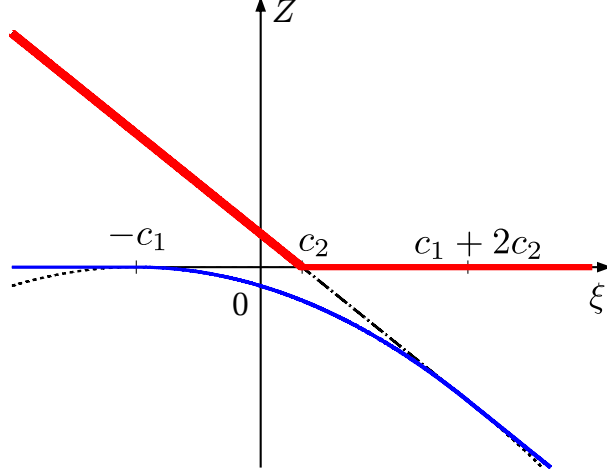


FIG. 2. The range of possible  $Z$  for each  $\xi$  indicated in Eq. (30). The upper and lower limits are shown by the bold red and thin blue curves, respectively. The dotted curve and chained line express  $Z = -(\xi + c_1)^2/[4(c_1 + c_2)]$  and  $Z = -\xi + c_2$ , respectively.

We regard  $\xi$  to be a variable parameter since it is controllable by the value of the static magnetic flux density. Further,  $Z$  is treated as another variable parameter because the initial values depend only on it. Therefore, it is farsighted to classify the time-evolution by the values of  $\xi$  and  $Z$ . The possible range of  $Z$  for each  $\xi$  is given by

$$\begin{cases} 0 \leq Z \leq -\xi + c_2 & (\xi \leq -c_1) \\ -\frac{(\xi+c_1)^2}{4(c_1+c_2)} \leq Z \leq -\xi + c_2 & (-c_1 \leq \xi \leq c_2) \\ -\frac{(\xi+c_1)^2}{4(c_1+c_2)} \leq Z \leq 0 & (c_2 \leq \xi \leq c_1 + 2c_2) \\ -\xi + c_2 \leq Z \leq 0 & (c_1 + 2c_2 \leq \xi). \end{cases} \quad (30)$$

The region is shown in Fig. 2.

## VII. CLASSIFICATION OF $\alpha$ FOR EVERY $\xi$ AND $Z$

There are three possible behaviors of  $\alpha$ , *i.e.*, keeps oscillating, converges to a certain value, and remains as the initial value. The values of  $\xi$ ,  $Z$ , and  $\alpha(0)$  determine the behavior.

In the case of oscillation, since  $P_1 P_2 \geq 0$  is necessary, we can classify the maximum value  $\alpha_M$  and minimum value  $\alpha_m$  in the following three subtypes  $O_1, O_2$ , and  $O_3$  given in Table I. Typical  $P_1$  and  $P_2$  for each subtype are shown in Fig. 3.

Subtype	$\alpha_m$	$\alpha_M$
$O_1$	$\alpha_{2-}$	$\alpha_{1-}$
$O_2$	$\alpha_{1+}$	$\alpha_{2+}$
$O_3$	$\alpha_{2-}$	$\alpha_{2+}$

TABLE I. The minimum and maximum values for each subtype of oscillating  $\alpha$ .

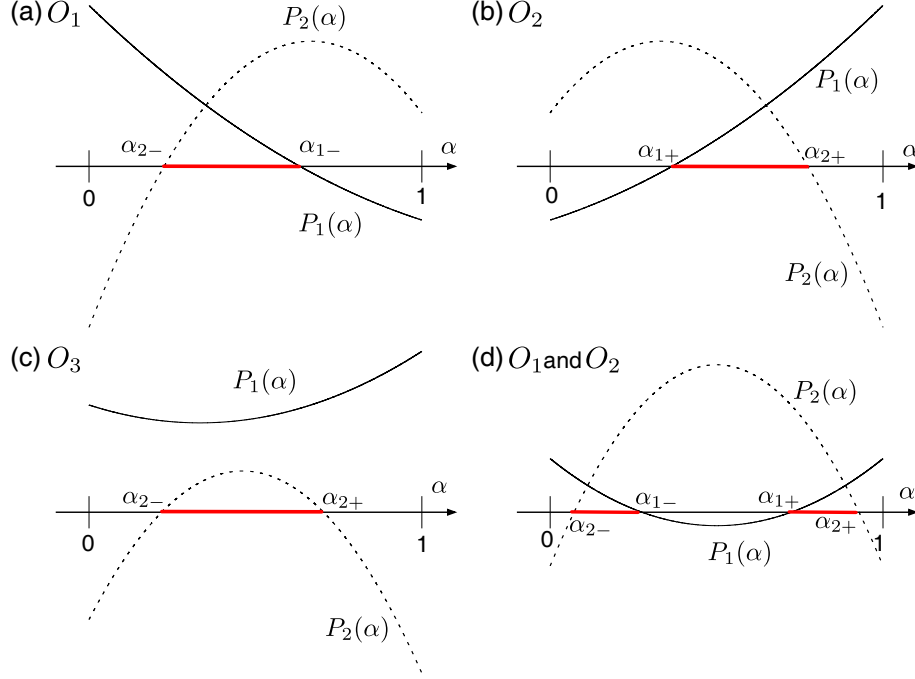


FIG. 3. Typical behaviors of  $P_1$  and  $P_2$  for the possible subtypes of oscillating  $\alpha$ . The zeros of  $P_1$  or  $P_2$  correspond to the maximum and minimum values of  $\alpha$  for each subtype. The range of  $\alpha$  is highlighted by the bold red lines. Both subtypes  $O_1$  and  $O_2$  are possible in the case of (d).

The subtype  $O_1$  is realized if

$$\begin{cases} -\xi + c_2 < Z < 0 & (c_2 < \xi) \\ Z = -\xi + c_2 & (c_2 < \xi < 2c_2) \\ -\frac{\xi^2}{4c_2} < Z < \min(0, -\xi + c_2) & (0 < \xi < 2c_2), \end{cases} \quad (31)$$

and  $\alpha_{2-} \leq \alpha(0) \leq \alpha_{1-}$  holds. In the first case, the condition for the initial value is auto-

matically satisfied. The subtype  $O_2$  is realized if

$$\begin{cases} 0 < Z < -\xi + c_2 & (\xi < c_2) \\ Z = 0 & (0 < \xi < c_2) \\ -\frac{\xi^2}{4c_2} < Z < \min(0, -\xi + c_2) & (0 < \xi < 2c_2), \end{cases} \quad (32)$$

and  $\alpha_{1+} \leq \alpha(0) \leq \alpha_{2+}$  holds. In the first case, the condition for the initial value is automatically satisfied. The subtype  $O_3$  is realized if

$$\begin{cases} -\frac{(\xi+c_1)^2}{4(c_1+c_2)} < Z < 0 & (-c_1 < \xi \leq 0) \\ -\frac{(\xi+c_1)^2}{4(c_1+c_2)} < Z < -\frac{\xi^2}{4c_2} & (0 < \xi < 2c_2) \\ -\frac{(\xi+c_1)^2}{4(c_1+c_2)} < Z < -\xi + c_2 & (2c_2 \leq \xi < c_1 + 2c_2), \end{cases} \quad (33)$$

where  $\alpha_{2-} \leq \alpha(0) \leq \alpha_{2+}$  holds necessarily.

In the case that  $\alpha$  converges, the limit value, initial condition, and range of  $\xi$  and  $Z$  are given by

$$\begin{cases} \alpha \rightarrow 0 & (\alpha(0) \neq 0 \wedge -c_1 < \xi \leq 0 \wedge Z = 0) \\ \alpha \rightarrow 1 & (\alpha(0) \neq 1 \wedge 2c_2 \leq \xi < c_1 + 2c_2 \wedge Z = -\xi + c_2) \\ \alpha \rightarrow \frac{\xi}{2c_2} & \left( \alpha(0) \neq \frac{\xi}{2c_2} \wedge 0 < \xi < 2c_2 \wedge Z = -\frac{\xi^2}{4c_2} \right), \end{cases} \quad (34)$$

where the symbol  $\wedge$  is a logical conjunction.

$\alpha$  does not change if its initial value and the range of  $\xi$  and  $Z$  satisfy

$$\begin{cases} \alpha(0) = 1 & (\forall \xi \wedge Z = -\xi + c_2) \\ \alpha(0) = 0 & (\forall \xi \wedge Z = 0) \\ \alpha(0) = \frac{\xi}{2c_2} & \left( 0 < \xi < 2c_2 \wedge Z = -\frac{\xi^2}{4c_2} \right) \\ \alpha(0) = \frac{\xi+c_1}{2(c_1+c_2)} & \left( -c_1 < \xi < c_1 + 2c_2 \wedge Z = -\frac{(\xi+c_1)^2}{4(c_1+c_2)} \right). \end{cases} \quad (35)$$

We have completely classified the behavior of  $\alpha$  for all possible  $\xi$  and  $Z$ . If  $\alpha$  is constant, there is nothing to do. If  $\alpha$  converges,  $\alpha'$  can change its sign at most once. Thus, all we have to do is to integrate the adequate square root of Eq. (28) at most twice. In the case of oscillating  $\alpha$ , the generalization of Jacobi's elliptic function is given in Appendix A and the solution can be obtained by a change of variable.

Note that if

$$0 < \xi < 2c_2 \wedge -\frac{\xi^2}{4c_2} < Z < \min(0, -\xi + c_2), \quad (36)$$

then both subtypes  $O_1$  and  $O_2$  are possible because the roots of  $P_1$  and  $P_2$  satisfy

$$0 < \alpha_{2-} < \alpha_{1-} < \alpha_{1+} < \alpha_{2+} < 1. \quad (37)$$

This is shown in Fig. 3(d). The initial value  $\alpha(0)$  determines which subtype is realized.

### VIII. SUFFICIENCY OF OBTAINING $\alpha$

Here we have solved  $\alpha$ . If it changes with time, it always satisfies  $0 < \alpha < 1$ . Let

$$\begin{aligned} \varphi_1(T) &= -(\Gamma_2 + 3\Gamma \mathcal{X})T - Z \int_0^T \frac{d\tau}{\alpha(\tau)}, \\ \varphi_2(T) &= \Phi - (\Gamma_1 + 3\Gamma \mathcal{X})T - (\xi - c_2 + Z) \int_0^T \frac{d\tau}{1 - \alpha(\tau)}, \end{aligned} \quad (38)$$

the four envelope functions are given as  $f = \sqrt{\alpha \mathcal{X}} \cos \varphi_1$ ,  $g = \sqrt{\alpha \mathcal{X}} \sin \varphi_1$ ,  $p = \sqrt{(1 - \alpha) \mathcal{X}} \cos \varphi_2$ , and  $q = \sqrt{(1 - \alpha) \mathcal{X}} \sin \varphi_2$ . Substituting them into Eq. (17) leads to

$$\begin{aligned} \mathbf{E}^{(1p)} &= \sqrt{\alpha \mathcal{X}} \begin{pmatrix} -\sin \theta \cos X \sin Y \\ \cos \theta \sin X \cos Y \\ 0 \end{pmatrix} \sin(T + \varphi_1) \\ &+ \sqrt{(1 - \alpha) \mathcal{X}} \sin X \sin Y \sin(T + \varphi_2) \mathbf{e}_z, \end{aligned} \quad (39)$$

where  $\mathbf{e}_z$  is the unit vector of the  $z$  direction. We can interpret  $\varphi_1$  and  $\varphi_2$  as the phase changes of each mode 1 and 2, respectively. The relative phase can be defined by  $\varphi_2 - \varphi_1$ . On the contrary to the nonlinear standing wave in a one-dimensional cavity [30], the relative phase continuously changes with time.

Since the analysis has been completed essentially, we describe the result in the physical context. We can interpret  $\alpha$  to express the intensity ratio between the two modes. Our analysis reveals that there are three possible types for the time evolution of  $\alpha$ , depending on the nonlinear parameters, direction of the standing waves, and static magnetic flux density. In the first type, the energy transfer continuously occurs between the two modes. The maximum and minimum ratios are further classified into three subtypes. In the second type, the energy transfer eventually decreases to zero and the mode ratio converges. In the third type, each mode keeps its initial energy.

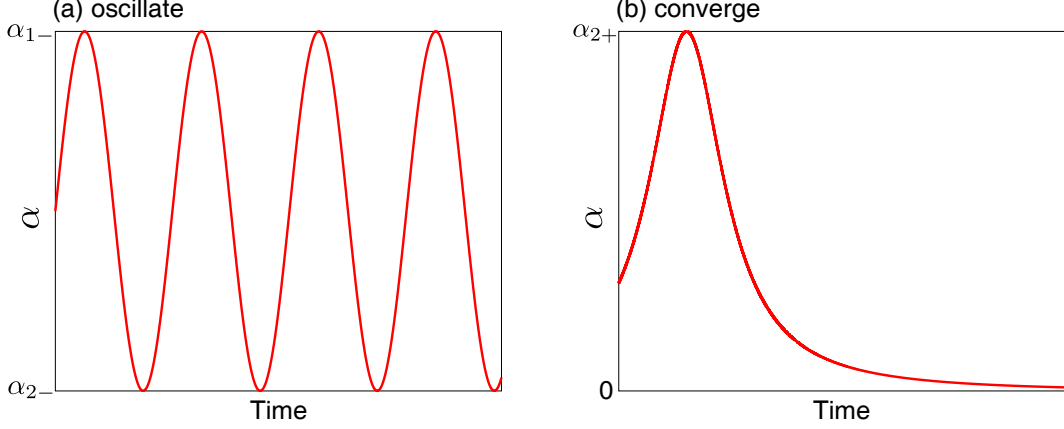


FIG. 4. Examples for oscillating and converging  $\alpha$ . (a) The oscillating subtype  $O_1$  is demonstrated.  $\xi$  and  $Z$  satisfy the third case in Eq. (31). The initial value is set to  $\alpha(0) = (\alpha_{1-} + \alpha_{2-})/2$  to meet the condition. (b) The converging type is demonstrated with the first case of Eq. (34) and  $\alpha'(0) > 0$ .

## IX. EXAMPLES OF $\alpha$

We give example of  $\alpha$  for the oscillating and converging types, as well as the electric field for a constant  $\alpha$ .

### A. Oscillating $\alpha$

In the case that  $\alpha$  oscillates, it is given by

$$\alpha = \frac{\alpha_M + \alpha_m}{2} + \frac{\alpha_M - \alpha_m}{2} \mathcal{S}(\sqrt{\mathcal{A}}T + T_0; \lambda_1, \lambda_2), \quad (40)$$

where the function  $\mathcal{S}$  is a generalization of Jacobi's elliptic function  $\text{sn}$  described in Appendix A. The constants  $\mathcal{A}$ ,  $\lambda_1$ , and  $\lambda_2$  are determined by the oscillation subtype.  $T_0$  depends on the oscillation subtype and the initial value. They are given in Appendix B.

### B. Converging $\alpha$

As aforementioned, we can obtain  $\alpha$  simply by integrating an adequate square root of Eq. (28). For the first case in Eq. (34),  $\alpha$  converges to zero. Let  $\bar{a} > 0$  be a certain constant,  $\alpha$

behaves at sufficiently large  $T$  as

$$\alpha \approx \bar{a} \exp \left[ -4(c_1 + c_2)c_2 \sqrt{-\alpha_1 - \alpha_2} T \right], \quad (41)$$

converges to zero.

### C. Constant $\alpha$

If  $\alpha$  is constant, the amplitudes of two modes are also constant. As examples, we show the solutions for the first and third cases of Eq. (35).

$A_2 = 0$  corresponds to the first case. Let

$$\Omega_1 = \Gamma_1 + 3\Gamma A_1^2, \quad (42)$$

we obtain  $\varphi_1(T) = -\Omega_1 T$  and

$$\mathbf{E}^{(\text{lp})} = A_1 \begin{pmatrix} -\sin \theta \cos X \sin Y \\ \cos \theta \sin X \cos Y \\ 0 \end{pmatrix} \sin(T - \Omega_1 T). \quad (43)$$

The third case is realized if and only if  $A_1 > 0$ ,  $A_2 > 0$ ,  $\cos \Phi = 0$ , and

$$(12C_{2,0} - C_{0,2})(A_1^2 - A_2^2) = 8(4C_{2,0} - C_{0,2})(B_{sx}^2 \sin^2 \theta + B_{sy}^2 \cos^2 \theta - B_{sz}^2). \quad (44)$$

Let

$$\Omega_3 = \Gamma_2 + 3\Gamma \mathcal{X} - \frac{\xi}{2}, \quad (45)$$

we obtain  $\varphi_1(T) = -\Omega_3 T$ ,  $\varphi_2(T) = \Phi - \Omega_3 T$ , and

$$\begin{aligned} \mathbf{E}^{(\text{lp})} = & A_1 \begin{pmatrix} -\sin \theta \cos X \sin Y \\ \cos \theta \sin X \cos Y \\ 0 \end{pmatrix} \sin(T - \Omega_3 T) \\ & + A_2 \sin \Phi \sin X \sin Y \cos(T - \Omega_3 T) \mathbf{e}_z. \end{aligned} \quad (46)$$

## X. DISCUSSION

We have demonstrated in the linear approximation that the uniform current generates an increasing correction of the second harmonic wave if  $\cos k\ell_1 = 0$  or  $\cos k\ell_2 = 0$  holds. It is of

interest to know whether the second harmonic is still generated when the leading part of the electromagnetic field differs from the classical term. To answer the question, it is sufficient to calculate a uniform current by applying the linear approximation for the leading part. The result is given by

$$\tilde{\mathbf{j}}_{\text{uni}} = -\frac{k}{4}(4C_{2,0} - C_{0,2})\mathcal{X} \sin 2\theta \sqrt{\alpha(1-\alpha)} \cos(2T + \varphi_1 + \varphi_2) \begin{pmatrix} B_{sy} \\ B_{sx} \\ 0 \end{pmatrix}. \quad (47)$$

Equation (11) is reproduced if the initial values are substituted. The time variations of  $\alpha$ ,  $\varphi_1$ , and  $\varphi_2$  are sufficiently slower than the period of one cycle  $2\pi/\omega$  and thus we can regard them to be constant in such a short timescale. Therefore, if  $\alpha$  does not rapidly converge to zero or unity, the second harmonic will keep increasing and become comparable to the classical term in the course of time. This consideration suggests that Eq. (17) is a good approximation in the timescale of  $t \lesssim \ell_1(A_1 + A_2)/[c(C_{2,0} + C_{0,2})(A_1 + A_2 + B_s)^3]$ . This value is, of course, much larger than the right-hand side in Eq. (16). Therefore, the validity of leading part calculation is unshaken.

## XI. FINAL REMARKS

We have analyzed the nonlinear electromagnetic wave in the two-dimensional rectangular cavity. The classical electromagnetic field is given as the two modes of standing wave and a constant magnetic flux density. Applying the linear approximation to calculate the corrective term in a short timescale, the result suggests that the leading part of the nonlinear electromagnetic wave has the same spatial distribution as the classical standing wave. Using this supposition, we derived nonlinear simultaneous differential equations which express the time evolution of the leading part. We introduced a new variable  $\alpha$  which expresses the intensity ratio of the two modes. The behavior of  $\alpha$  is classified into three types, *i.e.*, keep oscillating, converging, and constant. Once  $\alpha$  is obtained, the leading part of the nonlinear electromagnetic wave can be calculated immediately. It should be noted that the behaviors of the leading part in a long timescale is completely different between the two- and one-dimensional cavities. If we take the limits of  $\cos Y \rightarrow 1$  and  $\cos \theta \rightarrow 1$ , the leading part in Eq. (17) does not converge to the corresponding one-dimensional solution [30] while the classical term in Eq. (6) converges to a one-dimensional standing wave.

In the applicable range of linear approximation, we found a characteristic feature which has not appeared in the one-dimensional cavity system. In the two-dimensional cavity, the uniform current given in Eq. (11) or Eq. (47) can yield an increase of corresponding corrective term, if the cavity size satisfies  $\cos k\ell_1 = 0$  or  $\cos k\ell_2 = 0$ . The increased electromagnetic wave is a one-dimensional second harmonic. It increases with time but is not proportional to time, resulting in a slower growth than the resonant increase.

## ACKNOWLEDGMENTS

The author thanks Dr. M. Nakai and Dr. K. Mima for discussions on the nonlinear electromagnetic wave and its experimental application. The author quite appreciates Dr. J. Gabayno for checking the logical consistency of the text.

- 
- [1] W. Heisenberg and H. Euler, *Zeitschrift für Physik* **98**, 714 (1936).
  - [2] J. Schwinger, *Phys. Rev.* **82**, 664 (1951).
  - [3] M. Born, L. Infeld, and R. H. Fowler, *Proceedings of the Royal Society of London. Series A, Containing Papers on Mathematics and Physics* **188**, 101 (1945).  
<https://royalsocietypublishing.org/doi/pdf/10.1098/rspa.1934.0059>.
  - [4] E. H. Wichmann and N. M. Kroll, *Phys. Rev.* **101**, 843 (1956).
  - [5] V. I. Denisov, N. V. Kravtsov, and I. V. Krivchenkov, *Optics and Spectroscopy* **100**, 641 (2006).
  - [6] H. Carley and M. K.-H. Kiessling, *Phys. Rev. Lett.* **96**, 030402 (2006).
  - [7] S. H. Mazharimousavi and M. Halilsoy, *Foundations of Physics* **42**, 524 (2012).
  - [8] P. N. Akmansoy and L. G. Medeiros, *The European Physical Journal C* **78**, 143 (2018).
  - [9] I. TURCU, F. Negoita, D. Jaroszynski, P. Mckenna, S. Balascuta, D. Ursescu, I. Dancus, M. Cernaianu, M. TATARU, P. Ghenuche, D. STUTMAN, A. BOIANU, M. RISCA, M. Toma, C. PETCU, G. ACBAS, S. Yoffe, A. Noble, B. Ersfeld, and N. Zamfir, *Romanian Reports in Physics* **68**, S145 (2016).
  - [10] A. Di Piazza, C. Müller, K. Z. Hatsagortsyan, and C. H. Keitel, *Rev. Mod. Phys.* **84**, 1177 (2012).
  - [11] B. King and T. Heinzl, *High Power Laser Science and Engineering* **4**, e5 (2016).

- [12] G. A. Mourou, T. Tajima, and S. V. Bulanov, *Rev. Mod. Phys.* **78**, 309 (2006).
- [13] D. Eriksson, G. Brodin, M. Marklund, and L. Stenflo, *Phys. Rev. A* **70**, 013808 (2004).
- [14] G. Brodin, M. Marklund, and L. Stenflo, *Phys. Rev. Lett.* **87**, 171801 (2001).
- [15] S. N. Vlasov, *Radiophysics and Quantum Electronics* **58**, 497 (2015).
- [16] A. Arza and R. G. Elias, *Phys. Rev. D* **97**, 096005 (2018).
- [17] G. L. J. A. Rikken and C. Rizzo, *Phys. Rev. A* **63**, 012107 (2000).
- [18] K. Shibata, *The European Physical Journal D* **74**, 215 (2020).
- [19] K. Shibata, *The European Physical Journal D* **75**, 169 (2021).
- [20] G. Brodin, M. Marklund, and L. Stenflo, *Physica Scripta* **T98**, 127 (2001).
- [21] R. Ferraro, *Phys. Rev. Lett.* **99**, 230401 (2007).
- [22] V. I. Denisov and I. P. Denisova, *Optics and Spectroscopy* **90**, 282 (2001).
- [23] F. Della Valle, E. Milotti, A. Ejlli, G. Messineo, L. Piemontese, G. Zavattini, U. Gastaldi, R. Pengo, and G. Ruoso, *Phys. Rev. D* **90**, 092003 (2014).
- [24] F. D. Valle, G. D. Domenico, U. Gastaldi, E. Milotti, R. Pengo, G. Ruoso, and G. Zavattini, *Optics Communications* **283**, 4194 (2010).
- [25] G. Zavattini, F. D. Valle, U. Gastaldi, G. Messineo, E. Milotti, R. Pengo, L. Piemontese, and G. Ruoso, *Journal of Physics: Conference Series* **442**, 012057 (2013).
- [26] M. Bregant, G. Cantatore, S. Carusotto, R. Cimino, F. Della Valle, G. Di Domenico, U. Gastaldi, M. Karuza, V. Lozza, E. Milotti, E. Polacco, G. Raiteri, G. Ruoso, E. Zavattini, and G. Zavattini (PVLAS Collaboration), *Phys. Rev. D* **78**, 032006 (2008).
- [27] F. Della Valle, A. Ejlli, U. Gastaldi, G. Messineo, E. Milotti, R. Pengo, G. Ruoso, and G. Zavattini, *The European Physical Journal C* **76**, 24 (2016).
- [28] A. Cadène, P. Berceau, M. Fouché, R. Battesti, and C. Rizzo, *The European Physical Journal D* **68**, 16 (2014).
- [29] X. Fan, S. Kamioka, T. Inada, T. Yamazaki, T. Namba, S. Asai, J. Omachi, K. Yoshioka, M. Kuwata-Gonokami, A. Matsuo, K. Kawaguchi, K. Kindo, and H. Nojiri, *The European Physical Journal D* **71**, 308 (2017).
- [30] K. Shibata, *Phys. Rev. A* **104**, 063513 (2021).
- [31] J. Plebanski, *Lectures on non-linear electrodynamics: an extended version of lectures given at the Niels Bohr* (Copenhagen : NORDITA, 1970).
- [32] M. Fouché, R. Battesti, and C. Rizzo, *Phys. Rev. D* **93**, 093020 (2016).

- [33] R. Baier, A. Rebhan, and M. Wödlinger, *Phys. Rev. D* **98**, 056001 (2018).
- [34] K. Shibata, *Physica Scripta* **97**, 025506 (2022).